

Direct evidence of ferromagnetism without net magnetization observed by x-ray magnetic circular dichroism

S. Qiao,^{1,*} A. Kimura,^{2,†} H. Adachi,³ K. Iori,² K. Miyamoto,² T. Xie,² H. Namatame,¹ M. Taniguchi,^{1,2} A. Tanaka,⁴
T. Muro,⁵ S. Imada,⁶ and S. Suga⁶

¹*Hiroshima Synchrotron Radiation Center, Hiroshima University, Higashi-Hiroshima, Hiroshima 739-8526, Japan*

²*Graduate School of Science, Hiroshima University, Higashi-Hiroshima, Hiroshima 739-8526, Japan*

³*Institute of Materials Structure Science, KEK, Tsukuba, Ibaraki 305-0801, Japan*

⁴*ADSM, Hiroshima University, Higashi-Hiroshima, Hiroshima 739-8530, Japan*

⁵*Japan Synchrotron Radiation Research Institute, Sayo, Hyogo 679-5198, Japan*

⁶*Graduate School of Engineering Science, Osaka University, Osaka 560-8531, Japan*

(Received 14 July 2004; revised manuscript received 29 July 2004; published 26 October 2004)

We have performed x-ray magnetic circular dichroism experiments to study the cancellation of spin and orbital magnetic moments in (Sm,Gd)Al₂, a ferromagnet without net magnetization at a certain compensation temperature, T_{comp} . We verified the existence of long-range order for both spin and orbital magnetic moments at T_{comp} . The spin and orbital magnetic moments of the Sm ion are found always antiparallel coupled and the magnitude of its orbital magnetic moment is always larger than that of spin one, so the cancellation of magnetic moments cannot be achieved by only Sm 4*f* electrons. We show that the addition of spin magnetic moments of Gd ions and conduction electrons, which are ferromagnetically coupled with the spin magnetic moment of Sm ions, cancels out the surplus orbital magnetic moments in Sm ions completely and results in the zero magnetization at T_{comp} . All our experimental results can be reproduced well by atomic multiplet calculations.

DOI: 10.1103/PhysRevB.70.134418

PACS number(s): 75.50.Cc, 78.70.Dm

I. INTRODUCTION

Samarium atoms in solids usually contribute three electrons to the conduction band and the atoms become Sm³⁺ with the 4*f*⁵ configuration. The spin and orbital magnetic moments (M_S and M_L) of the Sm³⁺ ground state, which can be decided from Hund's rules as ⁶H_{5/2}, tend to cancel each other out because of their similar magnitudes and antiparallel orientation owing to the spin-orbital interaction,¹ and only a small surplus orbital magnetic moment is left. As a result, the contributions from conduction electrons and doped ions to the magnetism of samarium compounds become important.²⁻⁴ The tuning of the magnetic properties was demonstrated by Adachi and Ino such that the magnetization became zero at a certain compensation temperature, T_{comp} , when some of the samarium atoms in SmAl₂ were substituted with the gadolinium ones. They suggest that (Sm,Gd)Al₂ is a ferromagnet (with long-range order for both M_S and M_L) without net magnetization, as the total spin and orbital magnetic moments, including the contributions from Gd ions and conduction electrons, cancel each other out at T_{comp} .⁵ Their consideration is very direct and simple in that since the electron configuration of Gd³⁺ ion is 4*f*⁷, that is to say half-filled, its total orbital angular momentum is zero and only a spin magnetic moment is left, leading to the possibility of canceling out the surplus orbital magnetic moment in Sm³⁺. In this work, we verify this mechanism experimentally.

Although the existence of ferromagnetic ordering of M_S at T_{comp} (Ref. 6) and both M_S and M_L below and above T_{comp} (Ref. 7) was proved, the ferromagnetic ordering of M_L at T_{comp} has not been clearly observed, and no experimental measurement on the magnetic moments of dilute Gd ions has

been reported. Therefore, further quantitative studies for the individual behavior of M_S and M_L inside Sm and Gd ions are indispensable for confirming the ferromagnetic property completely and for understanding the mechanism of the zero net magnetization. X-ray magnetic circular dichroism (XMCD) is most suitable for this task because we can evaluate M_S and M_L separately by sum rules in an element-selective (Sm or Gd) and electronic-state-selective (the state of 4*f* or conduction electrons) manner through the tuning of the photon energy. In this work, the $M_{4,5}$ absorption edges are used, which give us information about the 4*f* electrons in Sm and Gd.

II. EXPERIMENT

The measurements were carried out at the beam line BL25SU of SPring-8 synchrotron radiation facility.⁸ A twin-helical undulator was adopted to generate left or right circularly polarized soft x rays with high (>99%) circular polarization. X-ray absorption spectra were measured in the total photoelectron yield mode. A magnetic field of 1.4 T was applied by permanent magnets normal to the sample surface. The XMCD spectrum is often obtained by taking the difference of absorption when reversing the sample magnetization. However for (Sm,Gd)Al₂, we have shown that this is not applicable near T_{comp} because of the insensitivity of the sample to external magnetic field due to its tiny magnetization.⁹ To resolve this problem, the XMCD needs to be observed by the difference of absorption caused by the reversing of helicity of incident photons. Our previous work shows that the 1.4 T magnetic field is not enough to saturate the sample magnetization and the degree of magnetization is not the same when magnetized at different temperatures be-

cause the sample is a polycrystal and its net magnetization is small.⁹ We note that even for nonferromagnetic materials, small XMCD can still be observed under an external magnetic field. To eliminate this possibility and to maintain the magnetization of the sample unchanged,¹⁰ which is important for the studies on temperature dependence of magnetic moments, in this work, the sample was magnetized in advance at a certain temperature T_m and the external magnetic field was removed before the measurements. We obtained the XMCD by taking the difference of two spectra in two successive scans. After the first scan the helicity of incident photons was reversed for the second scan. With this method, the accuracy of experimental data was not high enough to provide us with reliable information for understanding the mechanism of the cancellation of magnetic moments at T_{comp} .¹¹ The error is mainly caused by the time-dependent instability of the measurement system. If we can reverse the helicity of incident photons at every data point, this problem will be resolved. The twin helical undulator of SPring-8 BL25SU beam line has the capability of reversing the helicity of synchrotron radiation by the adjustment of local orbits in the straight section of the storage ring as fast as 10 Hz.¹² In this work, the XMCD measurements were done by this helicity-switching method with 1 Hz frequency. The helicity was reversed at every photon energy and the XMCD was measured as $\mu^+ - \mu^-$, where μ^+ and μ^- are the x-ray absorption coefficients with the helicity of the circular polarization parallel and antiparallel to the direction of the fixed magnetization orientation. The sample studied here is a $\text{Sm}_{0.982}\text{Gd}_{0.018}\text{Al}_2$ polycrystal ($T_{comp} \approx 81$ K), the same as that used in Ref. 5. Its surface was carefully scraped before every measurement to remove contamination.

III. DATA ANALYSIS

Although the linear dichroism of Sm^{3+} and Gd^{3+} is not zero, our calculation results have shown that the difference between $\int_{M_5+M_4} \frac{1}{2}(\mu^+ + \mu^-)$ and $\int_{M_5+M_4} \mu^0$ is less than 10% for Sm^{3+} and negligibly small for Gd^{3+} , where μ^0 is the absorption coefficient for linear polarized light with the polarization parallel to the quantization axis. Then the expectation values of M_L and M_S of the $4f$ electrons can be extracted from XMCD spectra by the sum rules¹³⁻¹⁵

$$\langle M_{LZ} \rangle = -\langle L_Z \rangle \mu_B = 2n \frac{\int_{M_5+M_4} (\mu^+ - \mu^-)}{\int_{M_5+M_4} (\mu^+ + \mu^-)} \mu_B,$$

$$\begin{aligned} \langle M_{SZ} \rangle &= -2\langle S_Z \rangle \mu_B \\ &= \left(2n \frac{\int_{M_5} (\mu^+ - \mu^-) - \frac{3}{2} \int_{M_4} (\mu^+ - \mu^-)}{\int_{M_5+M_4} (\mu^+ + \mu^-)} + 6\langle T_Z \rangle \right) \mu_B, \end{aligned}$$

where L_Z , S_Z , T_Z , and n are the orbital and spin angular momenta, magnetic dipole operator, and the number of holes in the $4f$ shell, respectively. The replacement of the integration of μ^0 by that of $\frac{1}{2}(\mu^+ + \mu^-)$ results in the same small relative error ($< 3\%$) for both spin and orbital magnetic moments (please note that $\langle T_Z \rangle$ is almost proportional to $\langle S_Z \rangle$ as shown in Table III), and this error can be absorbed by the

multiplying factor related to the unsaturated magnetization effect as discussed later. For rare-earth elements with less-than-half filled $4f$ shells, the off-diagonal term of the $3d-4f$ exchange interaction causes a large amount of $3d_{5/2}-3d_{3/2}$ mixing and the sum rule for M_S becomes invalid.¹⁶ Jo defined a correction factor X_I/X_E to describe the effect of this mixing, where

$$X_I = - \frac{\int_{M_5} (\mu^+ - \mu^-) - \frac{3}{2} \int_{M_4} (\mu^+ - \mu^-)}{\frac{3}{2} \int_{M_5+M_4} (\mu^+ + \mu^-)},$$

related to the absorption, and

$$X_E = \frac{2}{3n} \langle S_Z \rangle + \frac{2}{n} \langle T_Z \rangle.$$

For $3d$ electrons, $\langle T_Z \rangle$ is zero for polycrystal samples because of the decoupling between the quadrupolar charge distribution and magnetic spin orientation due to the small spin-orbital interaction¹⁷ and $\langle T_Z \rangle$ need not be considered. However, for $4f$ electrons, the crystal field is weaker than the spin-orbital interaction and $\langle T_Z \rangle$ is almost free of the crystal field¹⁸ and isotropic, so its value for polycrystal samples is about the same as that for free ions.

IV. RESULTS AND DISCUSSIONS

The $\text{Sm } M_{4,5}$ absorption and XMCD spectra obtained at different temperatures are shown in Fig. 1. Panel (c) shows the raw XMCD spectra with the sample being magnetized parallel and antiparallel to the sample surface normal. The near-zero constant background dichroism away from the absorption edges and the symmetry of these two spectra confirm that the systematic errors can be removed easily by background subtraction and the measurements can be done with the sample being magnetized along only one direction. At 81 K, the compensation temperature, both the spectra with T_m higher and lower than T_{comp} [see Fig. 1(d) and its caption] were taken, and the polarities of their dichroism are opposite to each other.

The XMCD measurements for Gd are somewhat difficult due to its small concentration. To remove the very high background dichroism, the measurement at every temperature was done by two scans with different magnetization directions, parallel and antiparallel to the sample normal. The average absorption and related XMCD spectra after background subtraction are shown in Fig. 2.

For atomic Sm^{3+} and Gd^{3+} ions, theoretical XMCD spectra and the expectation values of L_Z , S_Z , and T_Z of their $4f$ electrons were obtained from full atomic multiplet calculations. In our calculations, the electrostatic Coulomb and exchange parameters were taken from Ref. 19. The magnetic effect was introduced by a molecular field and its intensity at temperature T can be evaluated by solving the equation $B_m \mu_B = J_{ff} S B_S (2S \mu_B B_m / kT)$ where B_m , S , J_{ff} , $B_S(x)$ are the molecular field intensity, the spin angular momentum of the Sm^{3+} ground state (is $5/2$ here), the Heisenberg exchange parameter, and the Brillouin function, respectively. Our calculation results show that the slopes of the magnetic moment

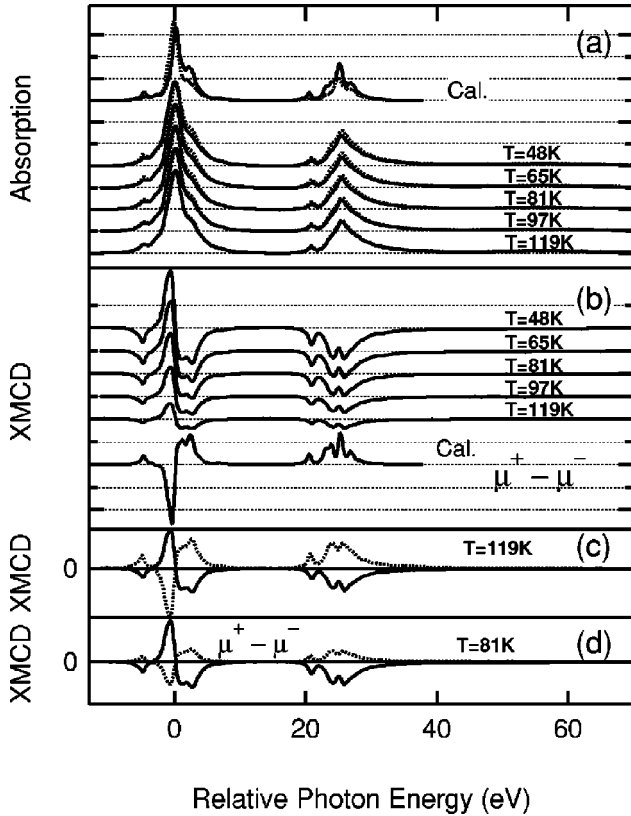


FIG. 1. (a) Sm $M_{4,5}$ x-ray absorption spectra observed at temperatures of 48, 65, 81, 97, and 119 K with $T_m=110$ K are compared with the theoretical spectra of atomic Sm^{3+} . Solid (broken) lines represent the absorptions with the helicity of the incident photons parallel (antiparallel) to the sample magnetization. (b) XMCD spectra deduced from the spectra in panel (a). (c) The experimental XMCD spectra taken at 119 K with the sample being magnetized parallel (solid line, $\mu^+ - \mu^-$) and antiparallel (broken line, $\mu^- - \mu^+$) to the sample normal with $T_m=110$ K. (d) XMCD spectra taken at 81 K with $T_m=110$ K [solid lines, deduced from the spectra in panel (a)] and $T_m=43$ K (broken line; the corresponding absorption spectra are not shown).

versus temperature [see Fig. 3(a)] are mainly determined by the molecular field intensity, whereas those of Sm^{3+} are a little bit reduced at low temperatures due to the crystal field. The best fitting between theoretical and experimental slopes is achieved when the crystal-field splitting between Γ_7 and Γ_8 levels of Sm^{3+} ground state is set as 2 meV, and the same J_{ff} of 0.96 meV, which is the half of that estimated from the sample Curie temperature T_C (about 130 K) as $J_{ff} = 3kT_C/[2S(S+1)]$, is adopted for both Sm^{3+} and Gd^{3+} ions because of the dilute concentration of Gd^{3+} . We can see that the experimental results can be reproduced very well by the theoretical calculations as shown in Fig. 3(a). The calculation results of relative energy level, the expectation values of spin and orbital angular momentum and magnetic dipole operator for the lowest multiplets of $4f$ electrons in atomic Sm^{3+} and Gd^{3+} ions when the molecular field is 2.25 meV (corresponding to the 48 K temperature; see Table III) are shown in Tables I and II, respectively. The strength of the molecular field estimated from above equations, the correction factor

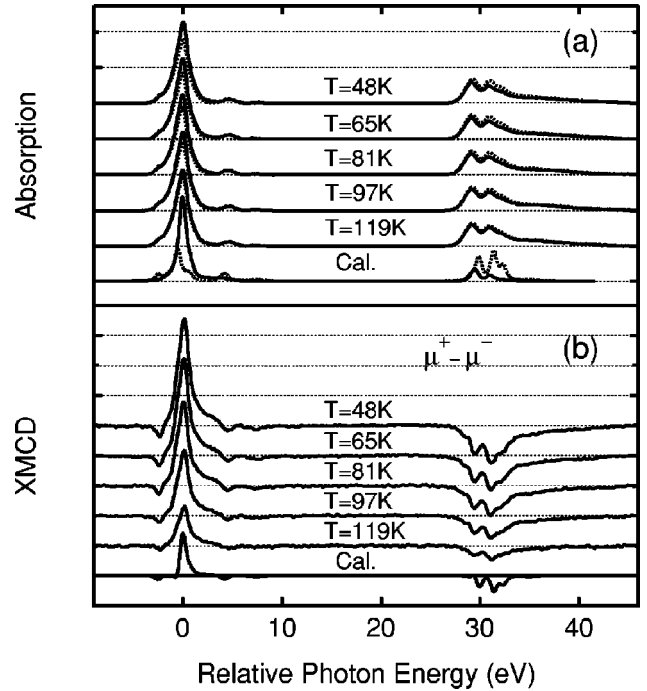


FIG. 2. (a) The average experimental spectra of Gd $M_{4,5}$ absorption with $T_m=110$ K are compared with the theoretical ones of atomic Gd^{3+} . The definition of solid and broken lines is the same as that in Fig. 1(a). (b) The XMCD spectra deduced from the spectra in panel (a).

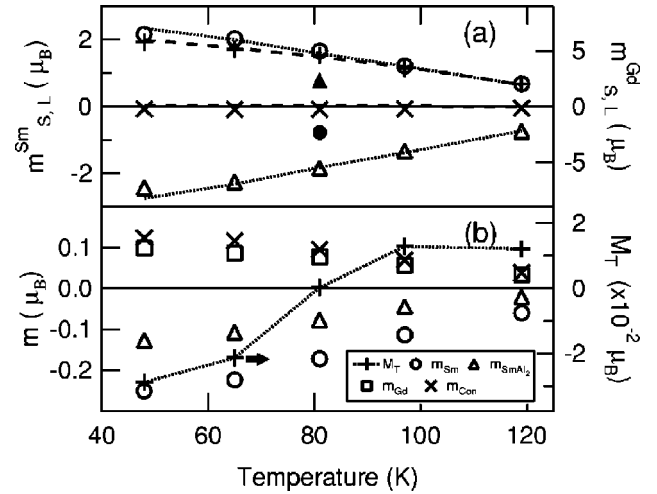


FIG. 3. (a) The experimental expectation values of m_s^{Sm} (\circ), m_L^{Gd} ($+$), m_L^{Sm} (Δ), and m_L^{Gd} (\times) (all enlarged by a factor of 3.05 to eliminate the unsaturated magnetization effect) when the sample was magnetized at 110 K (open marks) and 43 K (filled marks) are compared with theoretical estimations for atomic Sm (broken lines) and Gd (dashed lines) trivalent ions. (b) The distributions to the net magnetization ($+$, right axes) from the Sm ion (\circ), Gd ion (\square), and conduction electrons (\times) are shown with the net magnetization of SmAl_2 (Δ), which is the gross magnetic moments of both Sm ions and conduction electrons.

TABLE I. The calculation results of relative energy level, the expectation values of spin angular momentum, orbital angular momentum, and magnetic dipole operator for the lowest multiplets of 4f electrons in atomic Sm³⁺ when the molecular field is assumed to be 2.25 meV and the crystal-field splitting between Γ_7 and Γ_8 levels is set as 2 meV.

Energy (meV)	S_Z	L_Z	T_Z
0	-1.770	4.252	0.383
1.5	-1.155	2.643	0.233
6.4	-0.482	0.981	0.082
9.7	0.253	-0.753	-0.075
11.3	0.966	-2.449	-0.226
15.6	1.659	-4.147	-0.380
147.2	-0.618	4.103	0.321

X_I/X_E , and $\langle T_Z \rangle / \langle S_Z \rangle$ obtained from the multiplet calculations are listed in Table III.

Figure 3(a) summarizes the experimental spin and orbital magnetic moments of 4f electrons, denoted as m_S^{Sm} , m_L^{Sm} for Sm and m_S^{Gd} , m_L^{Gd} for Gd ions. They are extracted from the experimental XMCD spectra by the sum rules with corrections and using the parameters listed in Table III. Note that both m_S^{Sm} and m_L^{Sm} are not zero, showing the existence of ferromagnetic order, even at 81 K, which gives us direct experimental evidence that M_L of Sm 4f electrons in (Sm,Gd)Al₂ has ferromagnetic ordering at T_{comp} . Also we can see m_S^{Sm} and m_L^{Sm} are always aligned antiparallel as understood from the Hund's third rule. When $T_m > T_{\text{comp}}$ ($T_m < T_{\text{comp}}$), M_S is positive (negative) as shown by the open (filled) marks in Fig. 3(a), and that it is parallel (antiparallel) to the net magnetization. This agrees with other results,^{6,7} showing that the magnitude of the total spin magnetic moment is larger (smaller) than that of the total orbital one at the temperature higher (lower) than T_{comp} . This is also the reason for the opposite dichroism polarizations shown in Fig. 1(d). The larger temperature dependence of magnetic moments of Sm 4f electrons than that of Gd can be explained by the smaller size of effective g factor²⁰ [$=2(g-1)$] of the Sm³⁺ ground multiplet, which results in the narrower energy splitting between its manifold. From Fig. 3(a) we can see that the spin magnetic moments of Gd ions coupled ferromagnetically with those of Sm ions.

As a result of the different degree of sample magnetization at different T_m , as discussed before, the magnitude of experimental magnetic moments for $T_m=43$ K is much smaller than that for $T_m=110$ K [see Fig. 3(a)]. In Figs. 1(a) and 2(a), the difference of the theoretical μ^+ and μ^- is much larger than that of the experimental ones, because of the unsaturated magnetization of the sample. To eliminate the unsaturated magnetization effect, the experimental data in Fig. 3(a) are expanded by a factor of 3.05 to fit the theoretical results and they show the saturated (actual) magnetic moments in the sample. From Fig. 3, we can see $|m_L^{\text{Sm}}| > |m_S^{\text{Sm}}|$ holds in the whole temperature range, which agrees with the estimation made before for free Sm³⁺ ions¹

TABLE II. The calculation results of relative energy level, the expectation values of spin angular momentum, orbital angular momentum, and magnetic dipole operator for the lowest multiplets of 4f electrons in atomic Gd³⁺ when the molecular field is assumed to be 2.25 meV.

Energy (meV)	S_Z	L_Z	T_Z
0	-3.466	-0.034	0.010
4.5	-2.475	-0.025	0.007
8.9	-1.485	-0.015	0.004
13.4	-0.495	-0.005	0.001
17.9	0.495	0.005	-0.001
22.3	1.485	0.015	-0.004
26.8	2.475	0.025	-0.007
31.3	3.465	0.034	-0.010
3813.2	-2.344	-1.155	-0.185

and shows that the cancellation between spin and orbital magnetic moments cannot be achieved by only the Sm ions.

The experimental spectra and magnetic moments of 4f electrons can be reproduced quite well by the theoretical multiplet calculations for atomic Sm³⁺ and Gd³⁺ ions, which indicates that the behavior of the magnetic moments of 4f electrons in the sample can be well described by an atomic picture and the Sm and Gd ions here are mostly trivalent.

As the net magnetization is small, the magnetism of the sample depends strongly on the contribution from the conduction electrons. The magnetic moment of conduction electrons, m_{con} , of rare-earth compounds can be described as being caused by the exchange interaction between the 4f and conduction electrons, and thus its magnitude should be proportional to the spin magnetic moment of 4f electrons,² $m_{\text{con}} = C m_S^{\text{Sm}}$. The coefficient C can be determined from the experimental m_{con} of SmAl₂ ($0.21\mu_B$) (Ref. 21) and theoretical m_S^{Sm} ($3.61\mu_B$) both at 4.2 K; then the m_{con} at various temperatures can be deduced from the experimental m_S^{Sm} as shown in Fig. 3(b).

The contributions from different sources to the magnetism of Sm_{0.982}Gd_{0.018}Al₂ are shown in Fig. 3(b). When temperature decreases, the circular dichroism [see Figs. 1(b) and 2(b)], the sizes of magnetic moments [see Fig. 3(a)], and the net magnetic moments (vector sum of spin and magnetic moments) of every part [conduction electrons, Sm or Gd

TABLE III. The theoretical molecular field intensity, correction factor, and expectation value of magnetic dipole operator.

T (K)	B_m (meV)	$(X_I/X_E)_{\text{Sm}^{3+}}$	$(X_I/X_E)_{\text{Gd}^{3+}}$	$(T_Z/S_Z)_{\text{Sm}^{3+}}$	$(T_Z/S_Z)_{\text{Gd}^{3+}}$
48	2.25	3.13	0.912	-0.208	0.0099
65	2.11	2.95	0.912	-0.206	0.0099
81	1.92	2.91	0.912	-0.203	0.0099
97	1.64	2.84	0.912	-0.201	0.0099
119	1.00	2.74	0.913	-0.197	0.0099

ions; see Fig. 3(b)) all increase. The net magnetic moment of Sm^{3+} ions [\circ , $m_{\text{Sm}}=0.982(m_S^{\text{Sm}}+m_L^{\text{Sm}})$, where 0.982 is the Sm concentration] is always orbital dominant. The magnitude of m_{con} (\times) is not enough to cancel out the surplus orbital magnetic moment in Sm^{3+} and the net magnetic moment of SmAl_2 (\triangle , $m_{\text{SmAl}_2}=m_{\text{Sm}}+m_{\text{con}}$) cannot reach zero. The net magnetic moment of Gd ions [\square , $m_{\text{Gd}}=0.018(m_S^{\text{Gd}}+m_L^{\text{Gd}})$] is almost of spin kind only [the orbital one is negligibly small as shown in Fig. 3(a)] and its participation cancels out the surplus orbital magnetic moment completely. The total, or to say, the net magnetic moment of $(\text{Sm}, \text{Gd})\text{Al}_2$ ($+$, $M_T=m_{\text{Sm}}+m_{\text{con}}+m_{\text{Gd}}$) becomes zero at T_{comp} .

V. CONCLUSIONS

In conclusion, the existence of ferromagnetic ordering for both spin and orbital magnetic moments in $\text{Sm}_{0.982}\text{Gd}_{0.018}\text{Al}_2$ at the compensation temperature is proved perfectly by our XMCD study. The cancellation of spin and orbital magnetic

moments cannot be achieved by Sm ions only. The spin magnetic moment of conduction electrons is not enough to cancel out the surplus orbital magnetic moment in Sm ions and the addition of spin magnetic moment from Gd ions cancels out the orbital magnetic moment thoroughly at T_{comp} and results in the zero net magnetization. The magnetic moments of Sm and Gd ions in $(\text{Sm}, \text{Gd})\text{Al}_2$ can be well described in an atomic picture.

ACKNOWLEDGMENTS

We thank D. L. Feng and Ibrahim Kurash for their valuable suggestions for improving the phrasing of this paper. We also would like to thank Professor Takeo Jo for fruitful discussions on the applicability of sum rules to the rare earth ions. This work was partially supported by the Grant-in-Aid for Scientific Research from the Ministry of Education, Science, Sports and Culture, Japan, No. 13440113. This work was done under the approval of the SPring-8 Advisory Committee (Proposal 2003B06674-NSc-np-Na).

*Electronic address: qiaoshan@hiroshima-u.ac.jp

†Electronic address: akiok@hiroshima-u.ac.jp

¹The contributions of M_S and M_L to the paramagnetic moment of the free Sm^{3+} ion can be estimated to be $25\mu_B/\sqrt{35}$ and $-30\mu_B/\sqrt{35}$, respectively.

²A. M. Stewart, Phys. Rev. B **6**, 1985 (1972).

³H. Adachi, H. Ino, and H. Miwa, Phys. Rev. B **56**, 349 (1997).

⁴H. Adachi, H. Ino, and H. Miwa, Phys. Rev. B **59**, 11445 (1999).

⁵H. Adachi and H. Ino, Nature (London) **401**, 148 (1999).

⁶H. Adachi, H. Kawata, H. Hashimoto, Y. Sato, I. Matsumoto, and Y. Tanaka, Phys. Rev. Lett. **87**, 127202 (2001).

⁷J. W. Taylor, J. A. Duffy, A. M. Bebb, M. R. Lees, L. Bouchenoire, S. D. Brown, and M. J. Cooper, Phys. Rev. B **66**, 161319(R) (2002). It seems, however, that the direction of the sample magnetization was not well controlled in their experiment of x-ray diffraction, though this condition is crucial.

⁸Y. Saitoh, H. Kimura, Y. Suzuki, T. Nakatani, T. Matsushita, T. Muro, T. Miyahara, M. Fujisawa, K. Soda, S. Ueda, H. Harada, M. Kotsugi, A. Sekiyama, and S. Suga, Rev. Sci. Instrum. **71**, 3254 (2000).

⁹S. Qiao, A. Kimura, H. Adachi, T. Kambe, K. Yoshikawa, K. Yaji, C. Hirai, H. Sato, Y. Takeda, H. Namatame, M. Taniguchi, A. Tanaka, T. Muro, S. Imada, and S. Suga, Physica B **351**, 333 (2004).

¹⁰It seems the observed almost zero form factors near T_{comp} in Ref. 7 is the result of the unsuccessful control of the magnetization of their sample.

¹¹S. Qiao, A. Kimura, H. Adachi, K. Iori, K. Miyamoto, T. Xie, H. Namatame, M. Taniguchi, A. Tanaka, T. Muro, S. Imada, and S. Suga, J. Electron Spectrosc. Relat. Phenom. (to be published).

¹²T. Hara, K. Shirasawa, M. Takeuchi, T. Seike, Y. Saito, T. Muro, and H. Kitamura, Nucl. Instrum. Methods Phys. Res. A **498**, 496 (2003).

¹³B. T. Thole, P. Carra, F. Sette, and G. van der Laan, Phys. Rev. Lett. **68**, 1943 (1992).

¹⁴M. Altarelli, Phys. Rev. B **47**, 597 (1993).

¹⁵P. Carra, B. T. Thole, M. Altarelli, and X. Wang, Phys. Rev. Lett. **70**, 694 (1993).

¹⁶T. Jo, J. Electron Spectrosc. Relat. Phenom. **86**, 73 (1997).

¹⁷J. Stöhr, and H. König, Phys. Rev. Lett. **75**, 3748 (1995).

¹⁸The electronic states of Gd^{3+} is not influenced by the crystal field because its zero total orbital angular momentum. For Sm^{3+} , our calculations show that when the fourth- and sixth-order crystal-field parameters $A_4\langle r^4 \rangle$ and $A_6\langle r^6 \rangle$ change from 0 to 30 meV, $\langle T_z \rangle$ varies less than 0.8%.

¹⁹B. T. Thole, G. van der Laan, J. C. Fuggle, G. A. Sawatzky, R. C. Karnatak, and J.-M. Esteve, Phys. Rev. B **32**, 5107 (1985).

²⁰The Hamiltonian of the spin magnetic moment under the molecular field B_m can be expressed as $2\mu_B S_z B_m = 2(g-1)\mu_B J_z B_m$ (see Ref. 2).

²¹E. Belorizky, J. J. Niez, J. X. Boucherle, J. Schweizer, and P. M. Levy, J. Magn. Magn. Mater. **15-18**, 303 (1980). J. X. Boucherle, D. Givord, and J. Schweizer, J. Phys. (Paris) **43**, C7-199 (1982).